



University of
New Haven

University of New Haven
Digital Commons @ New Haven

Biology and Environmental Science Faculty
Publications

Biology and Environmental Science

7-24-2015

Biofilm Formation by *Borrelia burgdorferi* Sensu Lato

Venkata Arun Timmaraju
University of New Haven

Priyanka A.S. Theophilus
University of New Haven

Kunthavai Balasubramanian
University of New Haven

Shafiq Shakih
University of New Haven

David F. Luecke
University of New Haven

See next page for additional authors

Follow this and additional works at: <http://digitalcommons.newhaven.edu/biology-facpubs>

 Part of the [Biology Commons](#), and the [Ecology and Evolutionary Biology Commons](#)

Publisher Citation

Biofilm formation by *Borrelia burgdorferi* sensu lato. Venkata Arun Timmaraju, Priyanka A. S. Theophilus, Kunthavai Balasubramanian, Shafiq Shakih, David F. Luecke, Eva Sapi. FEMS Microbiology Letters Volume 362, Issue 15. DOI: <http://dx.doi.org/10.1093/femsle/fnv120> First published online: 24 July 2015

Comments

This is a pre-copyedited, author-produced PDF of an article accepted for publication in FEMS Microbiology Letters following peer review. The version of record of Venkata Arun Timmaraju, Priyanka A. S. Theophilus, Kunthavai Balasubramanian, Shafiq Shakih, David F. Luecke, Eva Sapi. Biofilm formation by *Borrelia burgdorferi* sensu lato FEMS Microbiology Letters Volume 362, Issue 15 is available online at: <http://dx.doi.org/10.1093/femsle/fnv120>.

Authors

Venkata Arun Timmaraju, Priyanka A.S. Theophilus, Kunthavai Balasubramanian, Shafiq Shakih, David F. Luecke, and Eva Sapi

Biofilm formation by *Borrelia sensu lato*

Arun Timmaraju^{1,2}□, Priyanka AS Theophilus¹□, Kunthavai Balasubramanian^{1,3}, Shafiq Shakih¹, David F. Leucke¹, Eva Sapi^{1*}

¹Lyme disease research group, Department of Biology and Environmental Science, University of New Haven, West Haven, CT, USA

²Present address: Interpace Diagnostics, New Haven, CT, 06519

³Present address: Department of Hematology, Yale School of Medicine, New Haven, CT, 06520

□ Contributed equally

* **Correspondence:** Eva Sapi Ph.D., Department of Biology and Environmental Sciences, University of New Haven, 1211 Campbell Avenue, Charger Plaza LL16. West Haven, CT, 06516, USA.
esapi@newhaven.edu

Keywords: *Borrelia burgdorferi*, *Borrelia afzelii*, *Borrelia garinii*, biofilm, Atomic force microscopy, EPS

Abstract

Bacterial biofilms are microbial communities held together by an extracellular polymeric substance matrix predominantly composed of polysaccharides, proteins and nucleic acids. We had previously shown that *Borrelia burgdorferi sensu stricto*, the causative organism of Lyme disease in the United States is capable of forming biofilms *in vitro*. Here, we investigated biofilm formation by *Borrelia afzelii* and *Borrelia garinii*, which cause Lyme disease in Europe. Using various histochemistry and microscopy techniques, we show that *Borrelia afzelii* and *Borrelia garinii* form biofilms, which resemble biofilms formed by *Borrelia burgdorferi sensu stricto*. High-resolution atomic force microscopy revealed similarities in the ultra-structural organization of the biofilms form by three *Borrelia* species. Histochemical experiments revealed a heterogeneous organization of exopolysaccharides among the three *Borrelia* species. These results suggest that biofilm formation might be a common trait of *Borrelia* genera physiology.

1. Introduction

Lyme Borreliosis is an infectious disease caused by spirochete bacteria of the genus *Borrelia* (Burgdorfer et al., 1982). *Borrelia burgdorferi sensu stricto* genospecies which includes several *Borrelia burgdorferi* strains is the main cause of Lyme disease in the United States, whereas members of the *Borrelia sensu lato* genospecies including *Borrelia afzelii* and *Borrelia garinii* have been shown to cause the disease in Europe (Hubálek and Halouzka, 1997; Rauter and Hartung, 2005). Although the three aforementioned *Borrelia* species are the major cause of Lyme disease, their remarkably vary in clinical disease manifestation. *Borrelia burgdorferi sensu stricto* infection is associated Lyme arthritis, whereas infection with *Borrelia afzelii* is associated with Acrodermatitis chronica atrophicans (ACA, cutaneous manifestation) and infection with *Borrelia garinii* is associated with neuroborreliosis (Wang et al., 1999).

37 The pleomorphic *Borrelia burgdorferi* spirochete interconverts among several morphological forms
38 including round body and cell wall deficient forms when exposed to altered environmental
39 conditions such as high ambient pH or temperature fluctuations (Preac-Mursic et al., 1989; Brorson
40 and Brorson, 1998; Mursic et al., 1996; Gruntar et al., 2001; Murgia and Cinco, 2004). In addition to
41 these forms, we previously reported that *Borrelia burgdorferi* sensu stricto strains B31 and 297 are
42 capable of forming biofilms *in vitro* (Sapi et al., 2012).

43 Biofilms are complex communities of free living planktonic microbes which shield constituent
44 individuals from hostile environments (Flemming and Wingender, 2010) and are characterized by
45 the presence of an extracellular polymeric substance (EPS). Biofilm EPS is typically composed of
46 polysaccharides, proteins, divalent metals and extracellular DNA, which serve various functions
47 (Flemming and Wingender, 2010; Stewart and Franklin, 2008; Sutherland, 2001; Branda et al.,
48 2005).

49 The various EPS components of the *Borrelia burgdorferi* sensu stricto biofilm are sulfated mucins,
50 non-sulfated mucins including alginate, extracellular DNA and calcium (Sapi et al., 2012). In the
51 present study, we analyzed potential biofilm formation by *Borrelia* sensu lato species *Borrelia afzelii*
52 and *Borrelia garinii* *in vitro*.

53 We observed that both *Borrelia afzelii* and *Borrelia garinii* are capable of biofilm formation when
54 grown at high cell densities. The *Borrelia afzelii* and *Borrelia garinii* biofilms resemble the biofilms
55 formed by *Borrelia burgdorferi* sensu stricto as evidenced by the presence of extracellular DNA,
56 calcium and a tower-like organization, however, they show a heterogeneous distribution in their
57 exopolysaccharide composition.

58 2. Materials and methods

59 Bacterial strains and culture conditions

60 Low passage isolates of *Borrelia burgdorferi* B31 (ATCC #35210, Burgdorfer et al., 1982), *Borrelia*
61 *afzelii* BO23 (ATCC #51992, Xu et al., 1995) and *Borrelia garinii* Fuji P1 (ATCC #51383, Baranton et
62 al., 1992) were obtained from American Type Culture Collection. Cells were maintained in Barbour-
63 Stoner-Kelly H (BSK-H, Sigma) media supplemented with 6% rabbit serum (Pel-Freeze) containing no
64 antibiotics in sterile 15 ml glass tubes and incubated at 33°C with 5% CO₂. Biofilm formation was
65 initiated by inoculating homogenous mid-log phase spirochetes (5×10^6 cells/ml) for one week in 4
66 well chamber glass (LAB-TEK) slides for histochemical staining experiments. Cultures were fixed with
67 ice cold 1:1 acetone-methanol for 15 minutes at room temperature (RT) prior to histochemical
68 staining experiments.

69 BacLight LIVE/DEAD staining

70 Cells were stained using a 1:1 mixture of LIVE/DEAD BacLight™ stain, a mixture of Syto9 and
71 Propidium Iodide stains (LIVE/DEAD BacLight™ Bacterial Viability Kit, Invitrogen) for 15 minutes
72 in the dark. The slides were coverslipped and images were acquired using fluorescent microscopy.
73

74 Crystal violet staining and quantitation

75 For crystal violet staining experiments, cells were cultured as above in 4-well chamber slides (LAB-
76 TEK) and fixed with ice cold 1:1 acetone-methanol. Post fixation, the cells were stained with crystal

77 violet (0.01% in PBS, Thermo Scientific) for 10 minutes. Slides were washed with 1x phosphate
78 buffer (PBS pH 7.4, Sigma) and imaged by bright field microscopy. For crystal violet biomass
79 quantitation, cells were cultured for one week in a 48 well plate, pelleted and washed with 500 μ l
80 PBS by centrifugation at 1650 g for 5 minutes. The resulting pellet was resuspended in 50 μ l of
81 0.01% crystal violet by vortexing and incubated at room temperature for 10 minutes. Crystal violet
82 was removed by centrifugation and washing with 500 μ l PBS at 1650 g for 5 minutes. The cell pellet
83 was resuspended in 200 μ l of 10% acetic acid by vortexing, followed by incubation in the dark at
84 room temperature for 15 minutes. Post incubation, the cells were pelleted at 1650 g for 5 minutes.
85 The supernatant was transferred to a 96-well plate and optical density was measured at 595 nm using
86 a BioTek spectrophotometer.

87

88 **MTT assay**

89 MTT (3-(4,5-dimethylthiazol-2-yl)-2,5-diphenyltetrazolium bromide) assay was performed as
90 previously described with brief modifications (Fallon and Hellestad, 2009). Bacteria were cultured
91 as described above for one week in a 48 well plate and incubated with 100 μ l of 2 mg/ml MTT in
92 PBS (Sigma) for 4 hours at 33°C in dark. Post incubation, the medium was centrifuged at 1500 g for 8
93 minutes to pellet the biofilm and solubilized using 150 μ l isopropanol for 20 minutes at RT. The
94 precipitate was pelleted at 3000 g for 8 minutes. The supernatant was transferred to a 96 well plate
95 and optical density was measured at 570 nm using a BioTek spectrophotometer.

96 **Total carbohydrate assay**

97 Total carbohydrate assay was performed as previously described with brief modifications (DuBois et
98 al., 1956). Cells were cultured for one week in a 48 well plate, pelleted and washed with 1ml PBS by
99 centrifugation at 1650 g for 5 minutes. To the pellet, 200 μ l of sterile distilled water was added and
100 resuspended by vortexing. Next, 100 μ l of 5% phenol was added, followed by addition of 500 μ l of
101 concentrated sulfuric acid. This mixture was incubated at 33°C for 20 minutes and optical density
102 was measured at 485 nm using a BioTek spectrophotometer.

103

104 **Statistical analysis**

105 Statistical analyses were performed using GraphPad Prism version 6.00 for Windows (GraphPad
106 Software, La Jolla California USA, www.graphpad.com). Quantitative data are presented as mean \pm
107 S.E. of three independent experiments, performed in triplicates. Differences between groups were
108 considered statistically significant at $p < 0.05$, compared using unpaired Student's t-test.

109

110 **Atomic force microscopy**

111 Biofilm rich stationary cultures were centrifuged at 6000 \times g for 5 minutes at room temperature and
112 the resultant cell pellets were gently resuspended in PBS and spotted onto Superfrost™ Plus slides
113 (Fisher). Contact mode AFM imaging in air was performed on a Nanosurf Easyscan 2 AFM
114 (Nanosurf) using qp-SCONT probes (Nanosensors Inc). Images were processed using Gwyddion
115 software (Nečas and Klapetek, 2012).

116 **Spicer and Meyer staining**

117 Spicer and Meyer sequential staining was performed as previously described (Spicer and Meyer,
118 1960; Sapi et al., 2012). First, fixed slides were stained aldehyde fuchsin solution (0.5% fuchsin
119 dye dissolved in 6% acetaldehyde in 70% ethanol with 1% concentrated hydrochloric acid) for 20
120 minutes, and dipped in 70% ethanol for 1 min and double distilled water for 1 minute. Next, slides
121 were stained with 1% Alcian blue in 3% acetic acid, pH 2.5 for 30 minutes, rinsed in double distilled

122 water for 3 minutes and passed through a chilled graded ethanol series (50%, 70% and 95% ethanol
123 for 3 minutes each) and dipped in chilled xylene for 2 minutes followed by mounting in Permount
124 (Fisher Scientific). Fuchsin and Alcian blue 8GX dyes were purchased from Sigma-Aldrich.

125 **Alginate immunofluorescence**

126 Immunofluorescent detection of alginate was performed as previously described (Sapi et al., 2012).
127 Briefly, fixed cells were blocked with 10% normal goat serum (Thermo Scientific) in PBS/0.5% bovine
128 serum albumin (BSA, Sigma) for 30 minutes at RT. Slides were then incubated with anti-alginate
129 rabbit polyclonal IgG antibody (1:100 dilution in dilution buffer - PBS pH 7.4+0.5% BSA) overnight in
130 a humidified chamber, followed by incubation with DyLight 594 conjugated goat anti-rabbit IgG
131 secondary antibody (1:200, Thermo Scientific) for 1 hour in at RT. Slides were then incubated with
132 FITC tagged *Borrelia* rabbit polyclonal IgG antibody (1:50, Thermo Scientific # PA1-73005) for 1 hour
133 at RT. Slides were then counterstained with 4',6-diamidino-2-phenylindole (DAPI, Sigma, diluted
134 1:1000 in PBS) and mounted with Permaflour (Fisher).

135 **Lectin binding analysis**

136 Fixed cells were washed with 0.1% BSA in PBS pH 7.4 and incubated with 20 ng/ml FITC conjugated
137 HHA and MOA lectins (EY Laboratories) for 2 hrs at RT in dark. Post incubation, slides were washed
138 with 0.1% BSA in PBS pH 7.4, counterstained with DAPI and mounted with Permaflour.

139 **Calcium staining**

140 Fixed cells were stained with 2% Alizarin Red-S (pH 4.2, Sigma) for four minutes at RT. Following
141 incubation, slides were washed twice using double distilled water, dehydrated through graded
142 alcohols and mounted using Permount (Fisher Scientific).

143 **Extracellular DNA staining**

144 Extracellular DNA was stained with 1 mM DDAO [7-hydroxy-9H-(1, 3-dichloro-9, 9 dimethylacridin-
145 2-one)] for 30 min at 37° C in dark. DDAO-treated slides were then washed two times using TE
146 buffer, counterstained with DAPI and mounted using Permaflour.

147 **Image acquisition and processing**

148 Images from histochemical staining experiments were acquired on a Leica DM2500 microscope with
149 a DFC500 camera. For fluorescent staining merged micrographs, raw images were sharpened to
150 remove lens blur using Photoshop CS6 (Adobe) and images from different channels were stacked
151 using ImageJ (NIH) and are displayed as maximum intensity z-projections.

152 **3. Results**

153 ***Borrelia burgdorferi*, *Borrelia afzelii* and *Borrelia garinii* form biofilms *in vitro***

154 We hypothesized that *Borrelia afzelii* and *Borrelia garinii* form biofilms when grown at a high cell
155 density, similar to the biofilms formed by *Borrelia burgdorferi* sensu stricto strains. To address this
156 question, we seeded mid log phase 5×10^6 *Borrelia afzelii* and *Borrelia garinii* cells and grew them for
157 one week under standard *Borrelia burgdorferi* B31 culture conditions of 33°C and 5% CO₂ in BSK-H
158 medium containing 6% rabbit serum (Sapi et al., 2012).

159 At the end of one week, cultures were observed by BacLight LIVE/DEAD staining and crystal violet
160 staining. Fluorescence micrographs of BacLight staining showed predominantly live cells, with some
161 dead cells in the aggregates formed by *Borrelia burgdorferi* B31, *Borrelia afzelii* and *Borrelia garinii*
162 (Figure 1 A-C). Bright field micrographs of crystal violet stained cultures show that *Borrelia afzelii*
163 and *Borrelia garinii* form biofilm like aggregates, surrounded by planktonic spirochetes similar to
164 the biofilms formed by *Borrelia burgdorferi* (Figure 1 D-F).

165 To quantitatively assess biofilm development, we performed the MTT and crystal violet assays to
166 analyze differences in growth kinetics and biomass of the aggregates formed by the three *Borrelia*
167 species. For these assays, 5×10^6 cells were grown in 48 well plates for one week and the total
168 contents of the well i.e. attached and floating biofilms, were harvested for analysis.

169 MTT assay revealed that *Borrelia garinii* has significantly low growth kinetics ($n=3$, $p \leq 0.05$)
170 compared to *Borrelia afzelii* and *Borrelia burgdorferi* B31, which do not differ in their growth rates
171 ($n=3$, $p \geq 0.05$) (Figure 1G). Crystal violet assay showed that the biomass between the three *Borrelia*
172 species did not differ significantly ($n=3$, $p \geq 0.05$) (Figure 1H).

173 **Ultra structural features of the *Borrelia* biofilms**

174 We and others have previously used atomic force microscopy (AFM) to study the internal
175 organization of bacterial biofilms (Oh et al., 2009; Cross et al., 2006; Sapi et al., 2012; Oh et al.,
176 2007). Here, we used contact mode AFM to get a closer look at the morphology and topography of
177 *Borrelia* aggregates.

178 Morphologically, compared to *Borrelia burgdorferi* B31 biofilms (Figure 2A), *Borrelia afzelii*
179 aggregates are composed of enmeshed spirochetes (Figure 2B, 3A), whereas *Borrelia garinii*
180 aggregates have a relatively higher proportion of round-bodies (Figure 2C, 3B). Furthermore,
181 aggregates formed by the three *Borrelia* species are organized as “towers”, with pits and
182 protrusions (Figure 2D-F, 3C) (Hall-Stoodley et al., 2008; Fey and Olson, 2010; Sapi et al., 2012)

183 Topographically, the tower organization of *Borrelia afzelii* and *Borrelia garinii* biofilm like aggregates
184 may be due to the presence of an extracellular polymeric substance (EPS) as observed in the case of
185 *Borrelia burgdorferi*. We estimated the EPS by measuring the heights of biofilm aggregates by
186 extracting the profiles of the scans from the AFM phase images and observed that the EPS heights
187 of *Borrelia* biofilm like aggregates of all three species are typically $\sim 1 \mu\text{m}$ tall. A representative x-y
188 surface plot shows the typical height profile and the presence of pits (Fig 3C) and protrusions across
189 aggregates formed by the three *Borrelia* species (Figure 2D-F).

190 **Are *Borrelia* aggregates true biofilms?**

191 All three *Borrelia* species grow as aggregates (Figure 1) and assemble an EPS as indicated by the
192 AFM peaks (Figure 2). To establish whether these aggregates are indeed biofilms, we studied the
193 various EPS components typically found in bacterial biofilms including mucins, carbohydrates,
194 calcium and extracellular DNA using various histochemical staining techniques.

Mucopolysaccharide rich matrix of *Borrelia* biofilms

195 To assess the presence of polysaccharides/ sugars in the biofilm EPS; we used Spicer & Meyer
196 Fuch sine-Alcian blue sequential histological staining method. This method has been extensively
197 used to study the mucin rich gastrointestinal tissues (Spicer and Meyer, 1960). Here, we use Spicer
198 & Meyer staining to differentiate between sulfated and non-sulfated/carboxylated. Representative
199 dark field micrographs show that *Borrelia burgdorferi* B31 aggregates are rich in non-
200 sulfated/carboxylated mucins (blue staining) in the center of the aggregates and are surrounded
201 possibly by sulfomucins and proteoglycans (fuchsia/ purple staining) (Figure 3A-B). *Borrelia afzelii*
202 (Figure 3C-D) and *Borrelia garinii* (Figure 3E-F) are rich in non-sulfated/carboxylated mucins in the
203 center of the aggregates but do not appear to be enriched for sulfomucins at the edges.
204 Interestingly, there is significant inter-species and intra-species heterogeneity in Spicer & Meyer
205 staining patterns, which did not correlate with biofilm sizes and adherence.
206

207 To assess whether there were any differences in the total carbohydrate secreted, we measured
208 carbohydrate content using the total carbohydrate assay. We observed that *Borrelia afzelii*
209 contained significantly more amounts of carbohydrates than *Borrelia burgdorferi* B31 ($n=3$, $p\leq 0.05$).
210 *Borrelia burgdorferi* and *Borrelia garinii*, and *Borrelia afzelii* and *Borrelia garinii* did not differ
211 significantly in carbohydrate content ($n=3$, $p\geq 0.05$) (Figure 3G).
212

213 Next, we looked at whether alginate, a non-sulfated mucopolysaccharide present in *Borrelia*
214 *burgdorferi sensu stricto* biofilms (Sapi et al., 2012), is present in *Borrelia afzelii* and *Borrelia garinii*
215 biofilm like aggregates. Immunofluorescent staining using the anti-alginate antibody showed the
216 presence of alginate in *Borrelia afzelii* and *Borrelia garinii* aggregates (Figure 4). This is consistent
217 with Spicer and Meyer staining indicating the presence of non-sulfated mucopolysaccharides.

218 These experiments suggest that *Borrelia afzelii* and *Borrelia garinii* also form muroid biofilms but
219 differ in the organization of the various mucins. We reasoned that the differences in Spicer and
220 Meyer staining may be due to the presence of other EPS polysaccharides.

221 *Pseudomonas aeruginosa* strains have three major EPS polysaccharides, namely Pel, Psl and alginate
222 with Pel and Psl playing important roles in biofilm attachment and development whereas alginate is
223 expressed only by muroid strains (Ma et al., 2007). To address whether the differences in the EPS
224 organization may be due to Psl polysaccharides, we used lectin-binding analyses.

225 Lectins are glycoproteins of animal, plant or microbial origin, which specifically bind carbohydrates
226 and have been used to identify various biofilm EPS components. Lectin HHA (from *Hippeastrum*
227 *hybrid*) and lectin MOA (from *Marasmius oreades*) have been used extensively to study the
228 presence of Psl exopolysaccharides in *Pseudomonas aeruginosa*. HHA lectin binds mannosyl units in
229 polysaccharides whereas MOA is a mushroom lectin which binds galactosyl residues on the ends of
230 glycan chains (Ma et al., 2007; Hall-Stoodley et al., 2008).

231 *Borrelia burgdorferi*, *Borrelia afzelii* and *Borrelia garinii* were stained with FITC conjugated HHA and
232 MOA lectins. Merged fluorescent micrographs of lectin staining (green) and DNA staining (blue). In
233 *Borrelia burgdorferi* B31 aggregates, HHA lectin staining was observed throughout the biofilm,
234 whereas in *Borrelia afzelii* and *Borrelia garinii*, HHA lectin staining was observed internal of the
235 biofilm (Figure 5 A-F). MOA lectin staining was observed throughout *Borrelia burgdorferi* B31 and
236 *Borrelia afzelii* aggregates, whereas in *Borrelia garinii* aggregates, MOA lectin staining was observed
237 at the periphery (Figure 5 G-L). These results indicate the presence of a Psl-like EPS, which may
238 interfere with the sulfomucin organization, leading to differences in Spicer-Meyer staining patterns
239 (Spicer and Meyer, 1960; Sapi et al., 2012).

240 **Presence of calcium in *Borrelia* biofilms**

241 Previously, we identified the presence of calcium in biofilms formed by *Borrelia burgdorferi sensu*
242 *stricto* strains (Sapi et al., 2012). To examine whether *Borrelia afzelii* and *Borrelia garinii* aggregates
243 also contain calcium, we used a calcium specific stain, Alizarin Red S. Merged dark field and
244 fluorescence micrographs revealed the presence of calcium in the aggregates formed by *Borrelia*
245 *afzelii* and *Borrelia garinii* but not on the surrounding spirochetes (Figure 6).

246 **Presence of extracellular DNA in *Borrelia* biofilms**

247 Another component of the EPS is extracellular DNA, which plays an important role in substrate
248 attachment and stabilization of biofilm. Using an eDNA specific stain DDAO, we show that the
249 aggregates formed by *Borrelia burgdorferi*, *Borrelia afzelii* and *Borrelia garinii* contain significant
250 amounts of eDNA, internal to the biofilm which is not found associated with isolated spirochetes,
251 however there are no differences in staining patterns among the three species (Figure 7 A-F).

252 **Discussion**

253 In this paper, we provide evidence that *Borrelia afzelii* and *Borrelia garinii* of the *Borrelia sensu lato*
254 genospecies can form biofilms *in vitro*. These biofilms are viable and are either surface adherent or
255 floating and show considerable heterogeneity in size and shapes, as observed for various biofilm
256 forming bacteria (Stewart and Franklin, 2008). Using atomic force microscopy coupled with
257 histochemical staining techniques, we identify similarities and differences in the biofilms formed by
258 the three species.

259 Quantitative experiments showed that *Borrelia burgdorferi* and *Borrelia afzelii* grow at a similar
260 rate, whereas the growth of *Borrelia garinii* is significantly slower. Despite the differences in growth
261 rates, the total biofilm biomass of the three species did not differ. Interestingly all three species
262 differ in their total carbohydrate content which suggest that they might produce different amounts
263 of extracellular polysaccharides.

264 Previously, we used atomic force microscopy (AFM) to characterize various stages in biofilm
265 formation by *Borrelia burgdorferi sensu stricto* (Sapi et al., 2012). Here, we used AFM to identify

266 potential morphological differences in the biofilm structures of different *Borrelia* species. Consistent
267 with our previous data, *Borrelia burgdorferi sensu stricto* forms a matrix-dense biofilm (Sapi et al.,
268 2012), whereas *Borrelia afzelii* forms a network-like biofilm and *Borrelia garinii* biofilm has a
269 relatively higher proportion of round-bodies.

270 Topographical analysis did not show any significant differences in the heights of different *Borrelia*
271 biofilms. These differences may not be characteristic of the biofilms formed these species, but may
272 be attributed to the differences in the diameters of the biofilm i.e. taller biofilm heights may
273 correspond to wider biofilm diameters irrespective of the bacteria being studied. Another
274 topographical feature of *Borrelia* biofilms is the presence of pits and protrusions, as observed in the
275 spirochete *Leptospira*, which forms biofilms by cell-cell aggregation (Triampo et al., 2004; Ristow et
276 al., 2008). Recently, it was reported that an unrelated bacterium, *Chromobacterium violaceum*
277 forms biofilms containing invaginations and extrusions that resemble the pits and protrusions of
278 *Borrelia* biofilms (Kamaeva et al., 2014).

279 The core of the EPS of the three *Borrelia* biofilms is rich in the non-sulfated/ carboxylated mucin -
280 alginate, indicating the presence of a mucoid biofilm. Alginate is a negatively charged polymer
281 which in the presence of divalent cations forms a gelatinous mucoid matrix (Remminghorst and
282 Rehm, 2006). In *Azotobacter* biofilms, alginate plays a protective role by maintaining capsule
283 structural integrity during unfavorable conditions (Clementi, 1997). In some strains of *Pseudomonas*
284 *aeruginosa*, the causative organism of cystic fibrosis, alginate is a major component of the mucoid
285 biofilm, which confers resistance to oxidative stress and host immune surveillance (Hentzer et al.,
286 2001).

287 We observed differences in the organization of sulfomucins around the biofilm edges of the three
288 *Borrelia* species. We reasoned that the differences might be due to the presence of a Psl-like
289 polysaccharide. Using lectin staining we identified that *Borrelia* biofilms are rich in mannose and
290 galactose and hence possess a Psl like polysaccharide as found in *P. aeruginosa* biofilms. (Ma et al.,
291 2007). However, the staining patterns of MOA and HHA lectins of *Borrelia* biofilms do not account
292 for the differences in sulfomucin staining.

293 The three *Borrelia* species studied here possess an EPS that contains Psl-like polysaccharide as well
294 as alginate, and *Borrelia* biofilms retain both Psl and alginate at maturation, unlike the mucoid *P.*
295 *aeruginosa* strains, which switch from Psl to alginate. Psl deletion mutants in mucoid *P. aeruginosa*
296 mucoid strains show deficiency in biofilm formation suggesting that the Psl polysaccharides are
297 required for biofilm formation and alginate expression is observed after stable biofilm adhesion (Ma
298 et al., 2006; Schurr, 2013). We suspect that a Psl-like polysaccharides secretion precedes alginate
299 secretion during *Borrelia* biofilm development.

300 Although the *Borrelia* biofilms show differences in polysaccharide organization and morphology,
301 they are similar in the organization of calcium and extracellular DNA. Calcium, plays a dual role by
302 stabilizing the alginate matrix and chelating eDNA, which increases biofilm matrix stability (Sapi et
303 al., 2012). Extracellular DNA is present internal to the *Borrelia* biofilm, consistent with its role in

304 facilitating biofilm formation (Whitchurch et al., 2002), intercellular adhesion (Vilain et al., 2009)
 305 and substrate attachment (Gloag et al., 2013). Furthermore, under altered physiological conditions,
 306 eDNA contributes to antimicrobial activity by chelating cations with its inherent negative charge
 307 (Mulcahy et al., 2008).

308 In summary, results obtained from this study indicate that the aggregates formed by *Borrelia afzelii*
 309 and *Borrelia garinii* are biofilms that resemble the biofilms formed by *Borrelia burgdorferi sensu*
 310 *stricto*. Taken together, we suggest that biofilm formation is a common trait for *Borrelia* genera,
 311 which could confer survival advantages during unfavorable conditions.

312

313 4. Acknowledgements

314 The study was supported by University of New Haven and grants from the Lymedisease.org, Tom
 315 Crawford's Leadership Children's Foundation, Midwest Lyme Foundation, National Philanthropic
 316 Trust and Warman Family to ES and an anonymous donor-advised fund of the NH Charitable
 317 Foundation to PAST. Microscopes used in this study were donated to the University of New Haven
 318 Lyme Disease Research Group by Lymedisease.org, Schwartz foundation, Lyme Research Alliance
 319 and Lyme Disease Association. The authors thank Dr. Gerald B. Pier, Harvard University for kindly
 320 donating the anti-alginate antibody. A part of this project involves work towards KB and SS's
 321 master's thesis.

322

323 5. Author contributions

324 AT, PAST, KB, SS and DFL performed the experiments. AT and ES designed the study, interpreted
 325 the data and wrote the manuscript.

326 6. References

327 Baranton, G., Postic, D., Saint Girons, I., Boerlin, P., Piffaretti, J. C., Assous, M., & Grimont, P. A.
 328 (1992). Delineation of *Borrelia burgdorferi sensu stricto*, *Borrelia garinii* sp. nov., and group VS461
 329 associated with Lyme borreliosis. *Int. J. Syst. Bacteriol.* 42: 378-383, 1992.

330 Branda, S. S., Vik, S., Friedman, L., and Kolter, R. (2005). Biofilms: the matrix revisited. *Trends*
 331 *Microbiol.* 13, 20–6. doi:10.1016/j.tim.2004.11.006.

332 Brorson, O., and Brorson, S. H. (1998). In vitro conversion of *Borrelia burgdorferi* to cystic forms in
 333 spinal fluid, and transformation to mobile spirochetes by incubation in BSK-H medium.
 334 *Infection* 26, 144–50.

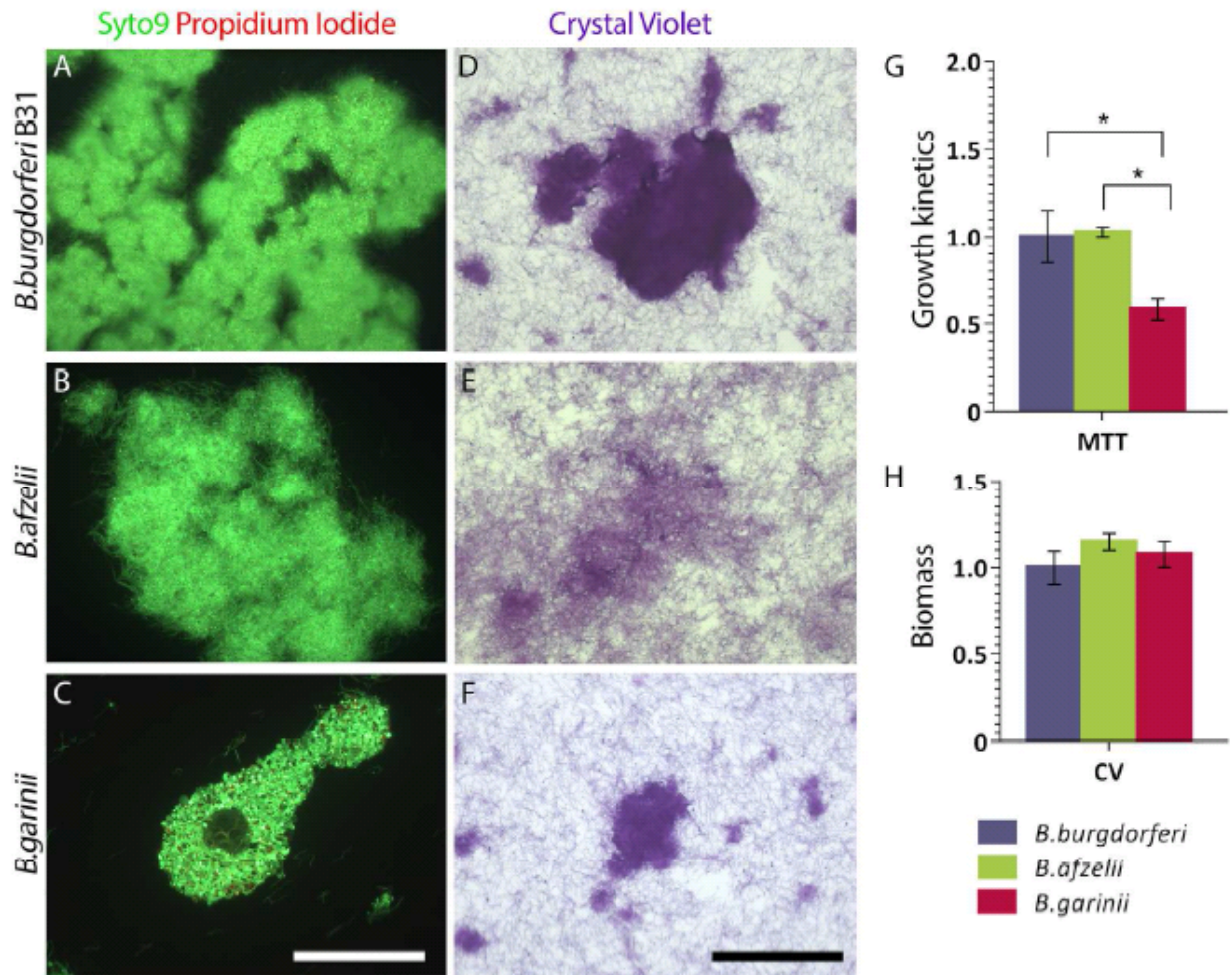
335 Burgdorfer, W., Barbour, A., Hayes, S., Benach, J., Grunwaldt, E., and Davis, J. (1982). Lyme disease-
 336 a tick-borne spirochetosis? *Science (80-)*. 216, 1317–1319. doi:10.1126/science.7043737.

- 337 Clementi, F. (1997). Alginate production by *Azotobacter vinelandii*. *Crit. Rev. Biotechnol.* 17, 327–61.
338 doi:10.3109/07388559709146618.
- 339 Cross, S. E., Kreth, J., Zhu, L., Qi, F., Pelling, A. E., Shi, W., and Gimzewski, J. K. (2006). Atomic force
340 microscopy study of the structure-function relationships of the biofilm-forming bacterium
341 *Streptococcus mutans*. *Nanotechnology* 17, S1–7. doi:10.1088/0957-4484/17/4/001.
- 342 DuBois, M., Gilles, K. a., Hamilton, J. K., Rebers, P. a., and Smith, F. (1956). Colorimetric Method for
343 Determination of Sugars and Related Substances. *Anal. Chem.* 28, 350–356.
344 doi:10.1021/ac60111a017.
- 345 Fallon, A. M., and Hellestad, V. J. (2009). Standardization of a colorimetric method to quantify
346 growth and metabolic activity of *Wolbachia*-infected mosquito cells. *In Vitro Cell. Dev. Biol.*
347 *Anim.* 44, 351–6. doi:10.1007/s11626-008-9129-6.
- 348 Flemming, H.-C., and Wingender, J. (2010). The biofilm matrix. *Nat. Rev. Microbiol.* 8, 623–33.
349 doi:10.1038/nrmicro2415.
- 350 Fey, P.D., and Olson M.E. (2010). Current concepts in biofilm formation of *Staphylococcus*
351 *epidermidis*. *Future microbiol*, 5:6: 917-933. doi:10.2217/fmb.10.56.
- 352 Gloag, E. S., Turnbull, L., Huang, A., Vallotton, P., Wang, H., Nolan, L. M., Mililli, L., Hunt, C., Lu, J.,
353 Osvath, S. R., et al. (2013). Self-organization of bacterial biofilms is facilitated by extracellular
354 DNA. *Proc. Natl. Acad. Sci. U. S. A.* 110, 11541–6. doi:10.1073/pnas.1218898110.
- 355 Gruntar, I., Malovrh, T., Murgia, R., and Cinco, M. (2001). Conversion of *Borrelia garinii* cystic forms
356 to motile spirochetes in vivo. *APMIS* 109, 383–8.
- 357 Hall-Stoodley, L., Nistico, L., Sambanthamoorthy, K., Dice, B., Nguyen, D., Mershon, W. J., Johnson,
358 C., Hu, F. Z., Stoodley, P., Ehrlich, G. D., et al. (2008). Characterization of biofilm matrix,
359 degradation by DNase treatment and evidence of capsule downregulation in *Streptococcus*
360 *pneumoniae* clinical isolates. *BMC Microbiol.* 8, 173. doi:10.1186/1471-2180-8-173.
- 361 Hentzer, M., Teitzel, G. M., Balzer, G. J., Heydorn, A., Molin, S., Givskov, M., and Parsek, M. R.
362 (2001). Alginate Overproduction Affects *Pseudomonas aeruginosa* Biofilm Structure and
363 Function. *J. Bacteriol.* 183, 5395–5401. doi:10.1128/JB.183.18.5395-5401.2001.
- 364 Hubálek, Z., and Halouzka, J. (1997). Distribution of *Borrelia burgdorferi* sensu lato genomic groups
365 in Europe, a review. *Eur. J. Epidemiol.* 13, 951–7.
- 366 Kamaeva, A. a, Vasilchenko, A. S., and Deryabin, D. G. (2014). Atomic Force Microscopy Reveals a
367 Morphological Differentiation of *Chromobacterium violaceum* Cells Associated with Biofilm
368 Development and Directed by N-Hexanoyl-L-Homoserine Lactone. *PLoS One* 9, e103741.
369 doi:10.1371/journal.pone.0103741.

- 370 Ma, L., Jackson, K. D., Landry, R. M., Parsek, M. R., and Wozniak, D. J. (2006). Analysis of
371 *Pseudomonas aeruginosa* conditional psl variants reveals roles for the psl polysaccharide in
372 adhesion and maintaining biofilm structure postattachment. *J. Bacteriol.* 188, 8213–21.
373 doi:10.1128/JB.01202-06.
- 374 Ma, L., Lu, H., Sprinkle, A., Parsek, M. R., and Wozniak, D. J. (2007). *Pseudomonas aeruginosa* Psl is a
375 galactose- and mannose-rich exopolysaccharide. *J. Bacteriol.* 189, 8353–6.
376 doi:10.1128/JB.00620-07.
- 377 Mulcahy, H., Charron-Mazenod, L., and Lewenza, S. (2008). Extracellular DNA chelates cations and
378 induces antibiotic resistance in *Pseudomonas aeruginosa* biofilms. *PLoS Pathog.* 4, e1000213.
379 doi:10.1371/journal.ppat.1000213.
- 380 Murgia, R., and Cinco, M. (2004). Induction of cystic forms by different stress conditions in *Borrelia*
381 *burgdorferi*. *APMIS* 112, 57–62.
- 382 Mursic, V. P., Wanner, G., Reinhardt, S., Wilske, B., Busch, U., and Marget, W. (1996). Formation and
383 cultivation of *Borrelia burgdorferi* spheroplast-L-form variants. *Infection* 24, 218–26.
- 384 Nečas, D., and Klapetek, P. (2012). Gwyddion: an open-source software for SPM data analysis. *Cent.*
385 *Eur. J. Phys.* 10, 181–188. doi:10.2478/s11534-011-0096-2.
- 386 Oh, Y. J., Jo, W., Yang, Y., and Park, S. (2007). Influence of culture conditions on *Escherichia coli*
387 O157:H7 biofilm formation by atomic force microscopy. *Ultramicroscopy* 107, 869–74.
388 doi:10.1016/j.ultramic.2007.01.021.
- 389 Oh, Y. J., Lee, N. R., Jo, W., Jung, W. K., and Lim, J. S. (2009). Effects of substrates on biofilm
390 formation observed by atomic force microscopy. *Ultramicroscopy* 109, 874–80.
391 doi:10.1016/j.ultramic.2009.03.042.
- 392 Preac-Mursic, V., Weber, K., Pfister, H. W., Wilske, B., Gross, B., Baumann, a, and Prokop, J. (1989).
393 Survival of *Borrelia burgdorferi* in antibioticly treated patients with Lyme borreliosis. *Infection*
394 17, 355–9.
- 395 Rauter, C., and Hartung, T. (2005). Prevalence of *Borrelia burgdorferi* Sensu Lato Genospecies in
396 *Ixodes ricinus* Ticks in Europe: a Metaanalysis Prevalence of *Borrelia burgdorferi* Sensu Lato
397 Genospecies in *Ixodes ricinus* Ticks in Europe: a Metaanalysis. 71.
398 doi:10.1128/AEM.71.11.7203.
- 399 Remminghorst, U., and Rehm, B. H. a (2006). Bacterial alginates: from biosynthesis to applications.
400 *Biotechnol. Lett.* 28, 1701–12. doi:10.1007/s10529-006-9156-x.
- 401 Ristow, P., Bourhy, P., Kerneis, S., Schmitt, C., Prevost, M.-C., Lilenbaum, W., and Picardeau, M.
402 (2008). Biofilm formation by saprophytic and pathogenic leptospire. *Microbiology* 154, 1309–
403 17. doi:10.1099/mic.0.2007/014746-0.

- 404 Sapi, E., Bastian, S. L., Mpoy, C. M., Scott, S., Rattelle, A., Pabbati, N., Poruri, A., Burugu, D.,
405 Theophilus, P. a S., Pham, T. V, et al. (2012). Characterization of biofilm formation by *Borrelia*
406 *burgdorferi* in vitro. *PLoS One* 7, e48277. doi:10.1371/journal.pone.0048277.
- 407 Schurr, M. J. (2013). Which bacterial biofilm exopolysaccharide is preferred, Psl or alginate? *J.*
408 *Bacteriol.* 195, 1623–6. doi:10.1128/JB.00173-13.
- 409 Spicer, S. S., and Meyer, D. B. (1960). Histochemical differentiation of acid mucopolysaccharides by
410 means of combined aldehyde fuchsin-alcian blue staining. *Tech. Bull. Regist. Med. Technol.* 30,
411 53–60.
- 412 Stewart, P. S., and Franklin, M. J. (2008). Physiological heterogeneity in biofilms. *Nat. Rev. Microbiol.*
413 6, 199–210. doi:10.1038/nrmicro1838.
- 414 Sutherland, I. (2001). Biofilm exopolysaccharides: a strong and sticky framework. *Microbiology* 147,
415 3–9.
- 416 Triampo, W., Doungchawee, G., Triampo, D., Wong-Ekkabut, J., and Tang, I.-M. (2004). Effects of
417 static magnetic field on growth of leptospire, *Leptospira interrogans* serovar canicola:
418 immunoreactivity and cell division. *J. Biosci. Bioeng.* 98, 182–6. doi:10.1016/S1389-
419 1723(04)00263-4.
- 420 Vilain, S., Pretorius, J. M., Theron, J., and Brözel, V. S. (2009). DNA as an adhesin: *Bacillus cereus*
421 requires extracellular DNA to form biofilms. *Appl. Environ. Microbiol.* 75, 2861–8.
422 doi:10.1128/AEM.01317-08.
- 423 Wang, G., Van Dam, A. P., Schwartz, I., & Dankert, J. (1999). Molecular typing of *Borrelia*
424 *burgdorferi* sensu lato: taxonomic, epidemiological, and clinical implications. *Clin microbiol rev,*
425 12(4), 633-653.
- 426 Whitchurch, C. B., Tolker-Nielsen, T., Ragas, P. C., and Mattick, J. S. (2002). Extracellular DNA
427 required for bacterial biofilm formation. *Science* 295, 1487.
428 doi:10.1126/science.295.5559.1487.
- 429 Xu, Y., & Johnson, R. C. (1995). Analysis and comparison of plasmid profiles of *Borrelia burgdorferi*
430 sensu lato strains. *J. Clin. Microbiol,* 33: 2679-2685.
- 431

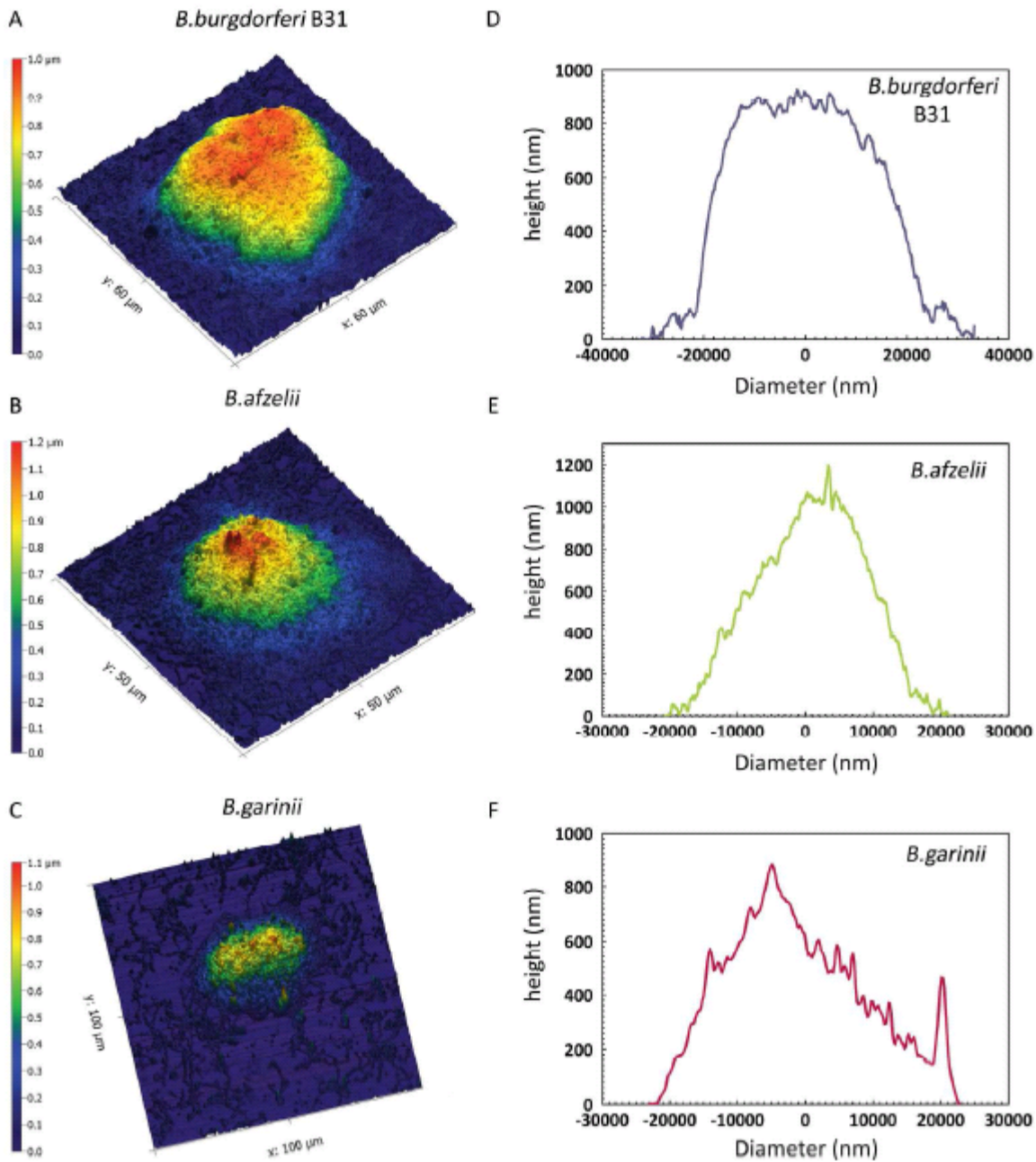
Figure legends



432

433 **Fig 1.** Biofilm like aggregate formation by *Borrelia* species. Panels A-C show fluorescent micrographs
 434 of LIVE/DEAD staining of floating *Borrelia* aggregates; Scale bar – 100 μ m and D-F show brightfield
 435 micrographs of crystal violet staining of attached *Borrelia* aggregates, surrounded by spirochetes;
 436 Scale bar – 200 μ m, of 5×10^6 cells of *Borrelia burgdorferi* B31 (A, D) *Borrelia afzelii* and (B, E) and
 437 *Borrelia garinii* (C, F) cultures grown for 1 week, respectively. Panels G-H show that the three
 438 *Borrelia* species grow at different rates (MTT assay), but do not differ in total biomass (Crystal violet
 439 assay) (n=3, *P \leq 0.05).

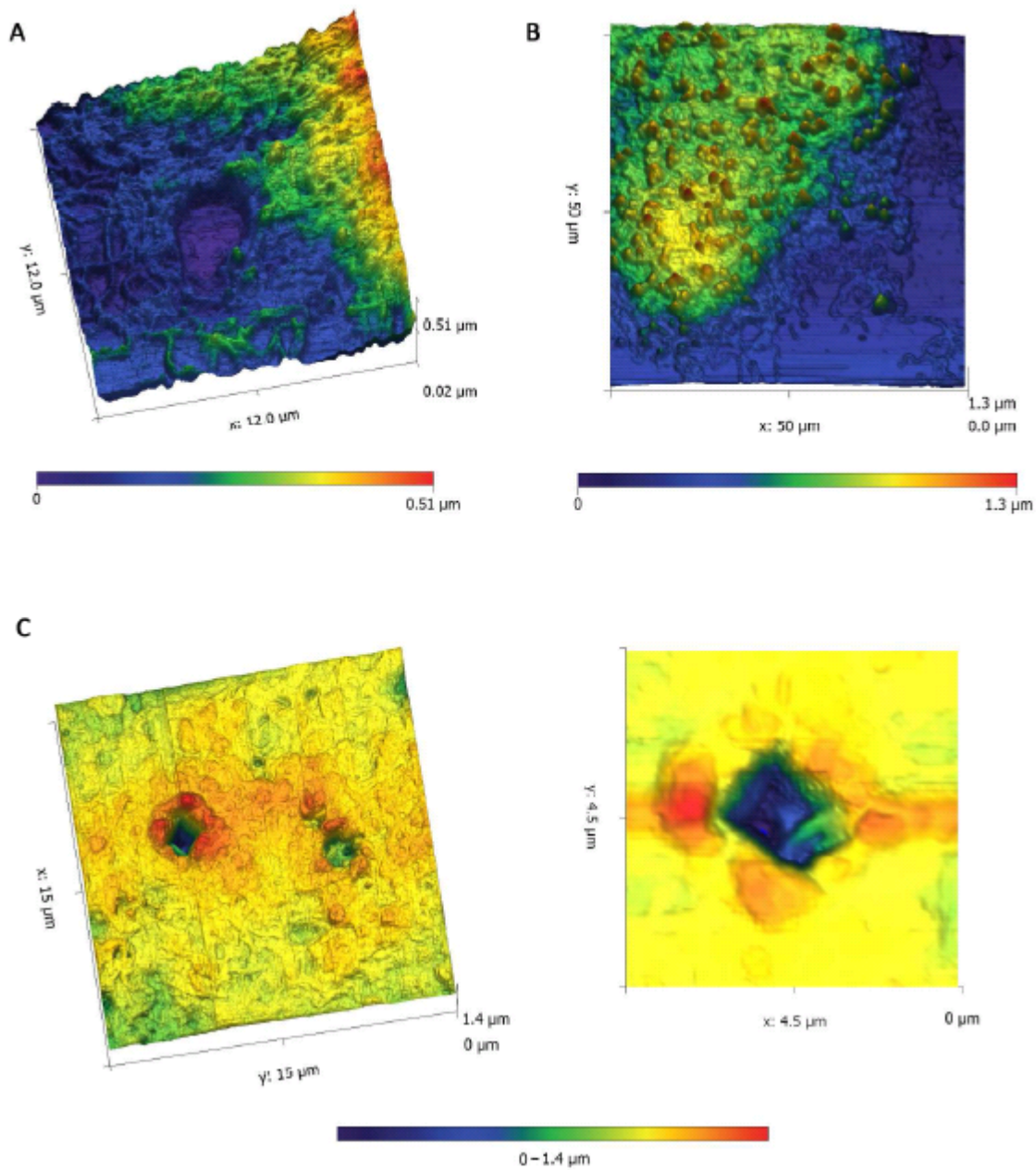
440



440

441 **Fig 2.** Ultrastructure of biofilm like aggregates formed by *Borrelia* species. Representative atomic
 442 force microscopy scans and profile graphs show ultrastructure and topology of (A, B) *Borrelia*
 443 *burgdorferi* B31 (C, D) *Borrelia afzelii* and (E, F) *Borrelia garinii* aggregates. AFM images shown here
 444 are pseudo-colored using Gwyddion software and the color gradient is a measure of height in μm .
 445 Graphs show x-y scatter plots of dry height corresponding-diameter measurements from AFM
 446 phase image profiles.

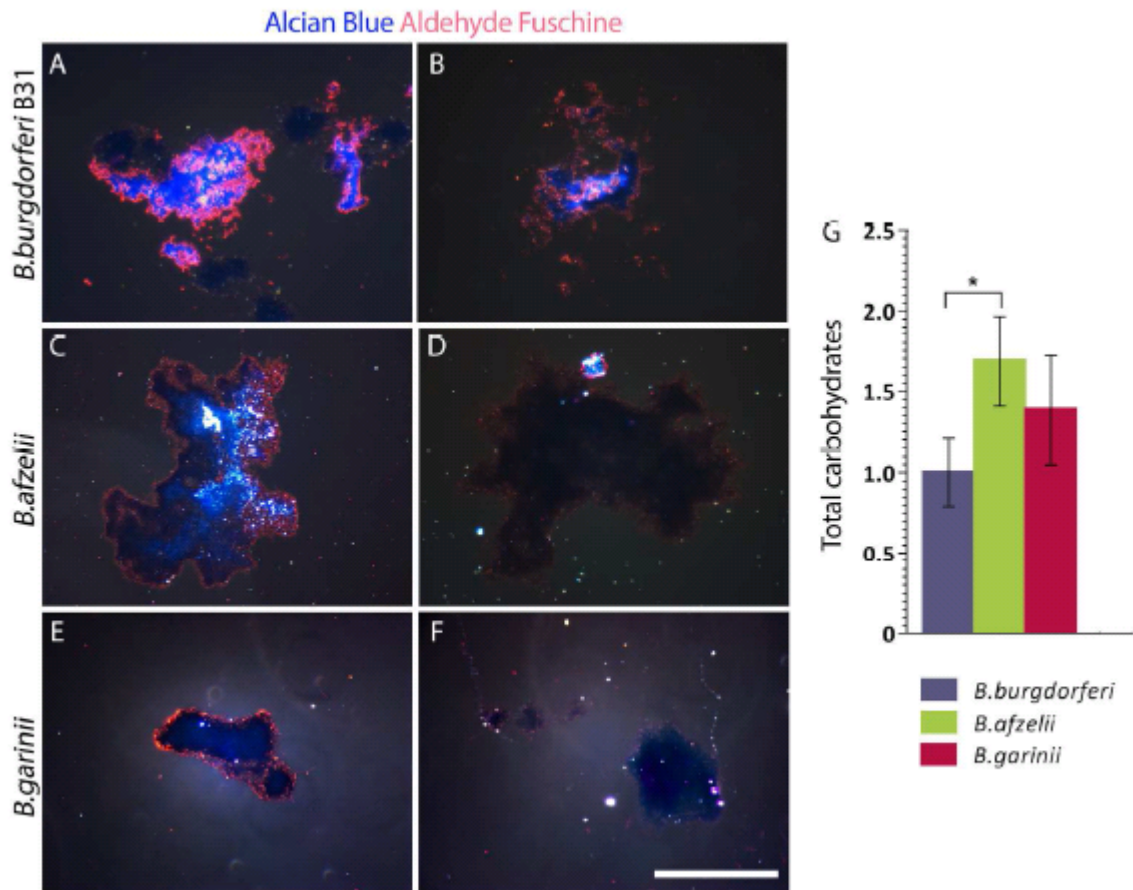
447



447

448 **Fig 3.** A-B) Atomic force micrographs of biofilm edges of *Borrelia afzelii* and *Borrelia garinii* show
 449 reticular networks and round-body enriched morphologies of the biofilms respectively. C) Higher
 450 resolution scans *Borrelia afzelii* biofilm showing a pit (invagination) deeper than 1 μm. AFM images
 451 shown here are pseudo-colored using Gwyddion software and the color gradient is a measure of
 452 height in μm.

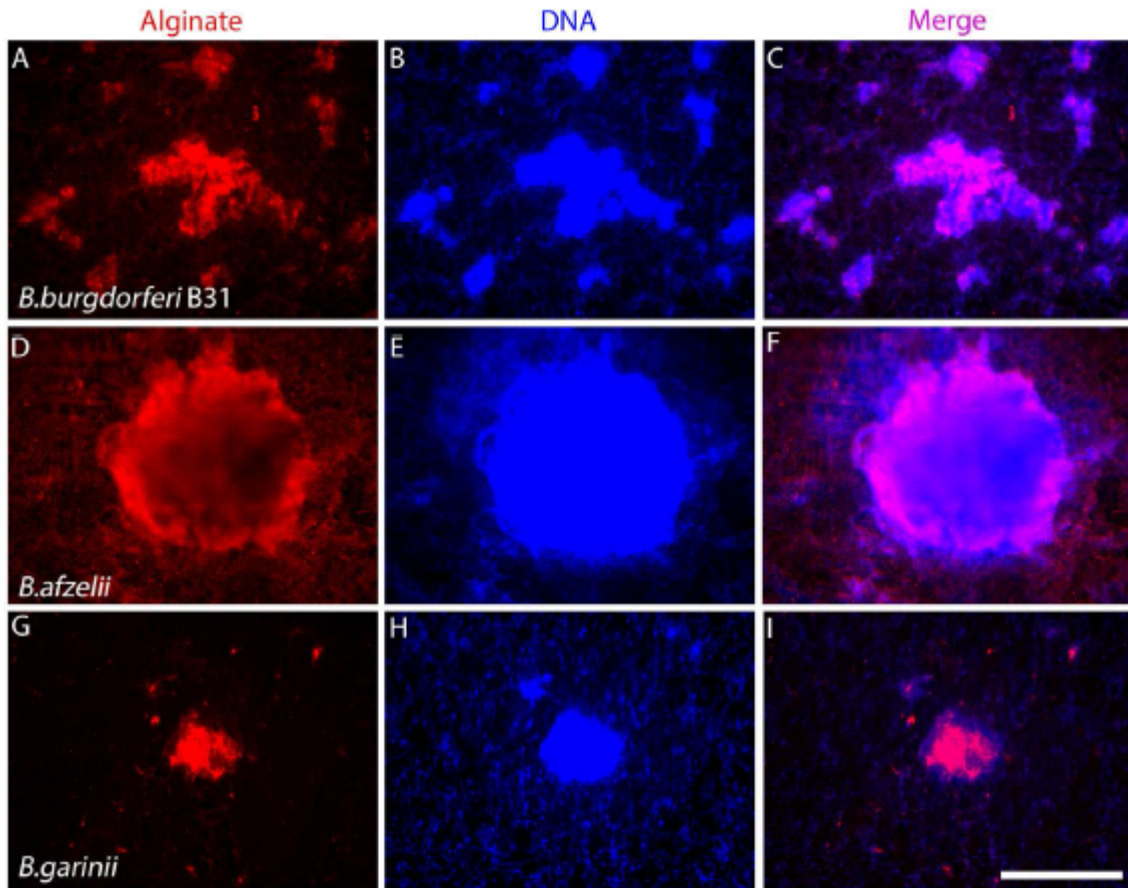
453



453

454 **Fig 4.** Mucoic phenotype of *Borrelia* aggregates. Representative dark field micrographs of
 455 sequential Spicer & Meyer staining show differences and heterogeneity in the mucin composition
 456 among aggregates formed by (A-B) *Borrelia burgdorferi* B31 (C-D) *Borrelia afzelii* and (E-F) *Borrelia*
 457 *garinii*. Scale bar - 100 μ m. Color index: Red/Fuchsia - weakly acidic sulfomucins; purple - strongly
 458 acidic sulfomucins and/or sulfated proteoglycans; blue - non-sulfated, carboxylated mucins. (G)
 459 *Borrelia* species grown for 1 week at high confluence differ in their total carbohydrate content as
 460 measured by total carbohydrate assay (n=3, * P<0.05).

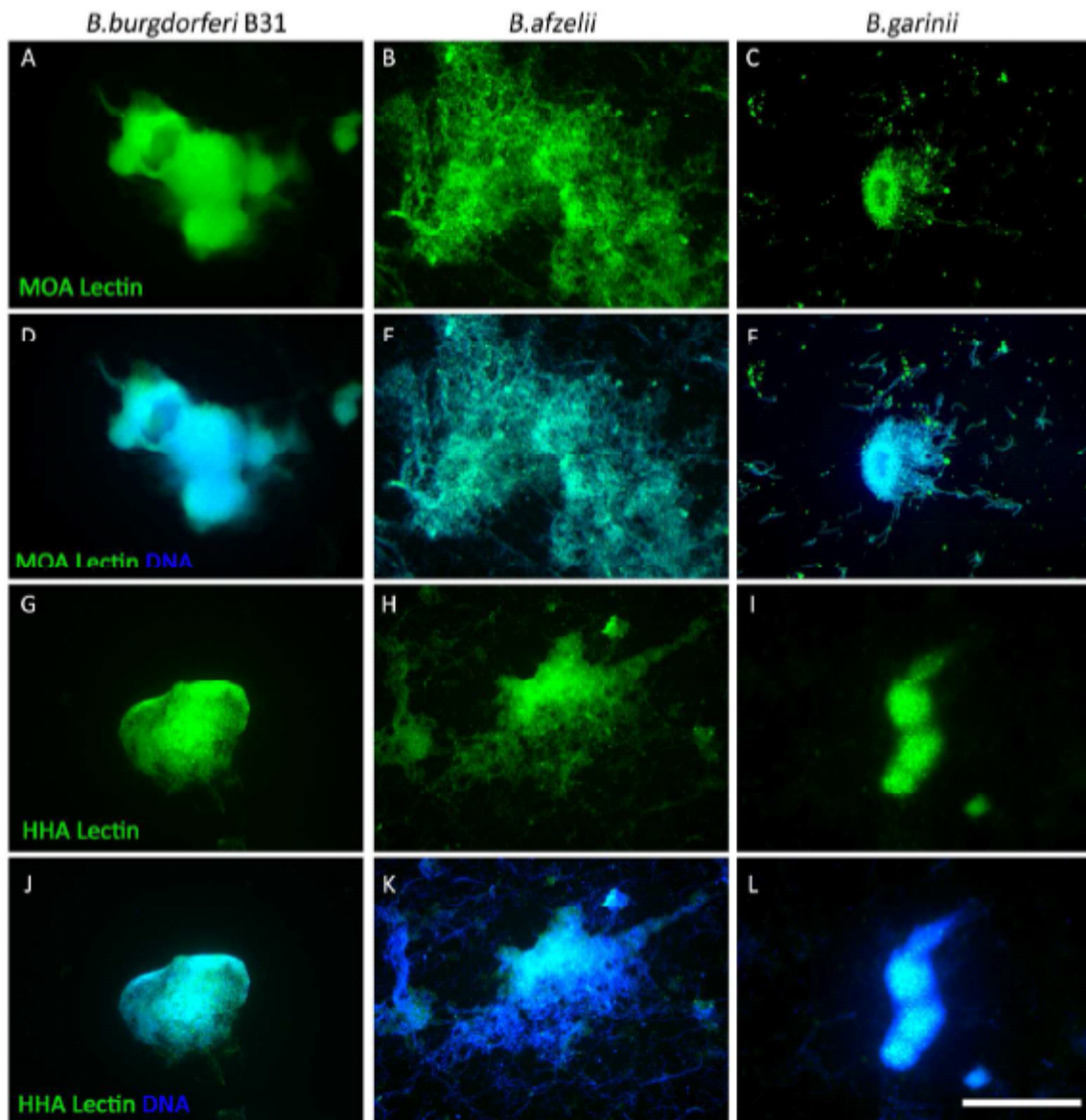
461



461

462 **Fig 5.** *Borrelia* aggregates contain an alginate rich matrix. Representative fluorescent micrographs A-
 463 C *Borrelia burgdorferi* B31, D-F *Borrelia afzelii* and G-I *Borrelia garinii* aggregates, with anti-alginate
 464 antibody (red) and DAPI (blue) and the respective merged maximum intensity projections show the
 465 presence of alginate rich EPS.

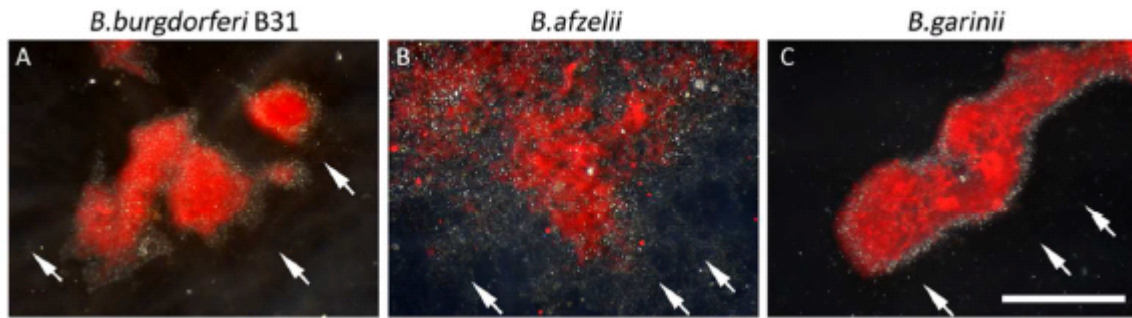
466



466

467 **Fig 6.** Borrelia aggregates contain a Psl-like polysaccharide. Representative fluorescent micrographs
 468 of (A, D, G, J) *Borrelia burgdorferi* (B, E, H, K) *Borrelia afzelii* and (C, F, I, L) *Borrelia garinii* aggregates
 469 stained with FITC conjugated HHA or MOA lectins (green) and DNA stained with DAPI (blue), show
 470 the presence of a Psl-like polysaccharide. Scale bar - 100 μ m.

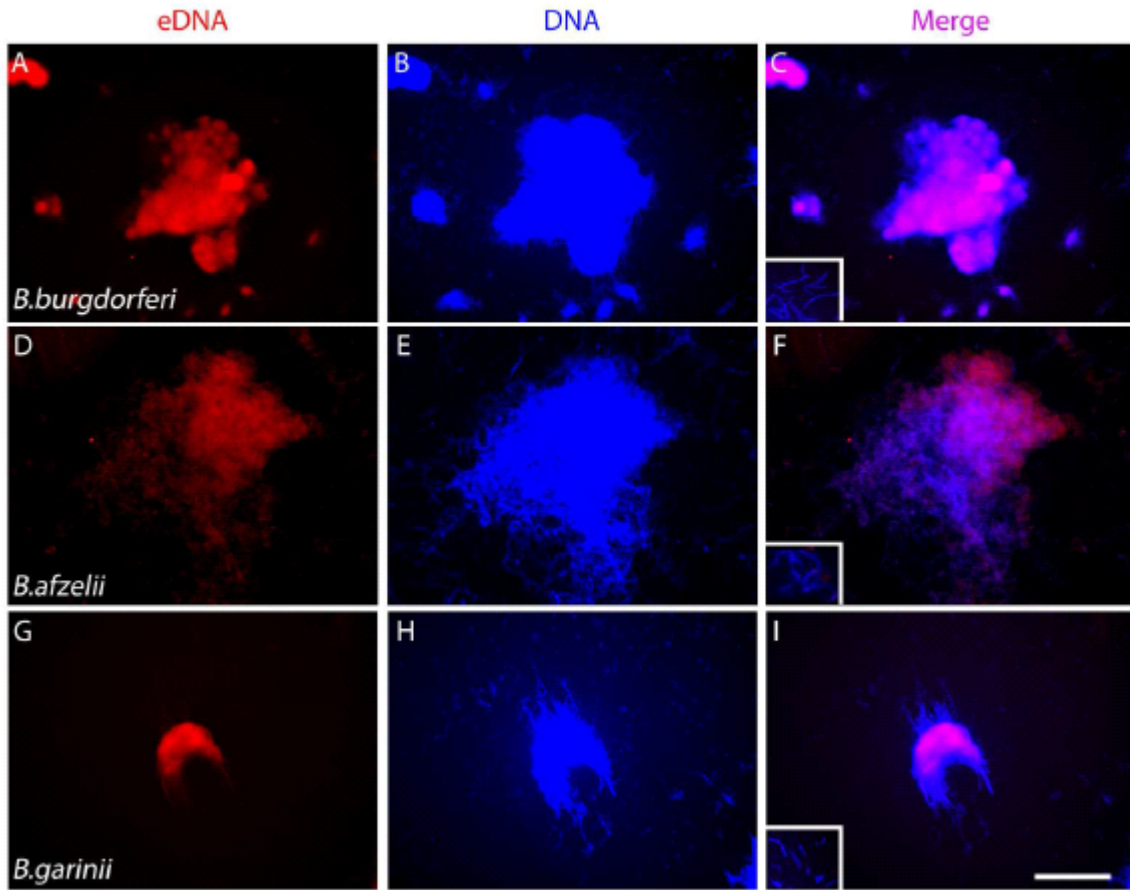
471



471

472 **Fig 7.** Presence of calcium in *Borrelia* aggregates. Representative dark field-fluorescence merged
473 micrographs of Alizarin red S staining shows localization of calcium (red) in aggregates formed by
474 (A) *Borrelia burgdorferi* (B) *Borrelia afzelii* and (C) *Borrelia garinii*. Scale bar - 100 μ m. Arrows show
475 that individual spirochetes surrounding the biofilm do not stain for alizarin red.

476



476

477 **Fig 8.** Presence of extracellular DNA in *Borrelia* aggregates but not in *Borrelia* spirochetes. Panels A-
 478 C show representative fluorescent micrographs of DDAO stained *Borrelia burgdorferi* B31, *Borrelia*
 479 *afzelii* and *Borrelia garinii* aggregates and spirochetes, respectively. DDAO eDNA staining – red, DAPI
 480 DNA staining – blue. Scale bar - 100 μ m. Inserts show individual spirochetes that do not stain for
 481 eDNA.

482